Photochemistry and Photobiology, 2006, 82: 834–843

Symposium-in-Print: UV Effects on Aquatic and Coastal Ecosystems

Ozone and UV Radiation over Southern South America: Climatology and Anomalies

S. Diaz*[1], C. Camilión[2], G. Deferrari[1], H. Fuenzalida[3], R. Armstrong[4], C. Booth[5], A. Paladini[6], S. Cabrera[7], C. Casiccia[8], C. Lovengreen[9], J. Pedroni[10], A. Rosales[10], H. Zagarese[11] and M. Vernet[12]

[1]Centro Austral de Investigaciones Científicas/Consejo Nacional de Investigaciones Científicas y Técnicas, Ushuaia, Argentina
[2]Centro Austral de Investigaciones Científicas/National Science Foundation/Inter American Institute for Global Change, Ushuaia, Argentina
[3]Universidad de Chile, Santiago, Chile,
[4]Universidad de Puerto Rico, Lajas, Puerto Rico
[5]Biospherical Instruments Inc., San Diego, CA
[6]Instituto de Investigaciones en Ingeniería Genética y Biología Molecular/Consejo Nacional de Investigaciones Científicas y Técnicas, Buenos Aires, Argentina
[7]Universidad de Chile, Santiago, Chile
[8]Universidad de Magallanes, Punta Arenas, Chile
[9]Universidad Austral de Chile, Valdivia, Chile
[10]Universidad de la Patagonia San Juan Bosco, Trelew, Argentina
[11]Instituto Tecnológico de Chascomús, Consejo Nacional de Investigaciones Científicas y Técnicas–Universidad Nacional de General San Martín, Chascomús, Argentina
[12]Scripps Institution of Oceanography, Integrative Oceanographic Division, University of California San Diego, La Jolla, CA

Received 26 September 2005; accepted 12 April 2006; published online 13 April 2006 DOI: 10.1562/2005-09-26-RA-697

ABSTRACT

Ozone and UV radiation were analyzed at eight stations from tropical to sub-Antarctic regions in South America. Ground UV irradiances were measured by multichannel radiometers as part of the Inter American Institute for Global Change Radiation network. The irradiance channels used for this study were centered at 305 nm (for UV-B measurements) and 340 nm (for UV-A measurements). Results were presented as daily maximum irradiances, as monthly averaged, daily integrated irradiances and as the ratio of 305 nm to 340 nm. These findings are the first to be based on a long time series of semispectral data from the southern region of South America. As expected, the UV-B channel and total column ozone varied with latitude. The pattern of the UV-A channel was more complex because of local atmospheric conditions. Total column ozone levels of <220 Dobson Units were observed at all sites. Analysis of autocorrelations showed a larger persistence of total column ozone level than irradiance. A decreasing cross-correlation coefficient between 305 and 340 nm and an increasing cross-correlation coefficient between 305 nm and ozone were observed at higher latitudes, indicating that factors such as cloud cover tend to dominate at northern sites and that ozone levels tend to dominate at southern sites. These results highlight the value of long-term monitoring of radiation with multichannel radiometers to determine climatological data and evaluate the combination of factors affecting ground UV radiation.

INTRODUCTION

After the discovery of depletion in the stratospheric ozone levels during the spring in Antarctica in the mid-1980s (1), the study of the variability of UV-B radiation at the earth's surface became a topic of great interest for the atmospheric sciences community. Biologists, physicians and epidemiologists studying the effect of UV-B on the environment and on human health expressed the need for accurate UV irradiance values and doses for their studies (2–5). In response to this need investigators have measured UV radiation with a variety of instruments, from broadband to spectral, at individual stations and throughout networks (6–9).

South America is a region of particular interest for this type of study because of its proximity to the Antarctic ozone hole. During spring, when the area of the ozone hole increases and the stratospheric vortex elongates, the southern tip of South America is often under the influence of the ozone hole. After the vortex breaks, ozone-depleted air masses from Antarctica pass over the region. This area is more affected by depleted ozone levels than any other region (6–8) and few studies have investigated this phenomenon in detail (10–12). We present an 8 year time-series analysis (from 1995 through 2002) of UV radiation measured by a network of eight multichannel instruments distributed from the Tropic of Capricorn to Tierra del Fuego. The radiometers used in this network perform simultaneous measurements at five channels cen-

*Corresponding author email: subediaz@speedy.com.ar (S. Diaz)

Table 1. Sites, geographic coordinates, altitude, date of starting operation or period considered in this study and total number of days in the period.*

Region (country)	Lat, long; elevation	Study period	Duration of study period (days)
La Parguera (Puerto Rico)	17°58.224′N, 67°02.723′W; 16 m	Since 1 January 1995	—
San Salvador de Jujuy (Argentina)	24.17°S, 65.02°W; 1300 m	1 January 1995–31 December 2002	2574
Buenos Aires (Argentina)	34.58°S, 58.47°W; sea level	1 January 1995–31 December 2002	2840
Santiago de Chile (Chile)	33.41°S, 70.65°W; sea level	1 January 1995–31 December 2002 (Except 1997)	1473
San Carlos de Bariloche (Argentina)	41.01°S, 71.42°W; 700 m	7 August 1998–31 December 2002	1307
Valdivia (Chile)	39.81°S, 73.25°W; sea level	1 January 1995–31 December 2002	2536
Puerto Madryn–Playa Unión (Argentina)	43.3°S, 65.05°W; sea level	1 January 1995–31 December 2002	2492
Trelew (Argentina)	43.25°S, 65.31°W; sea level	1 January 1995–31 December 2002	2492
Trelew 2 (Argentina)	43.25°S, 65.31°W; sea level	Since 1 January 1999	—
Punta Arenas (Chile)	53.09°S, 70.55°W; sea level	1 January 1995–31 December 2002 (except 1997)	2014
Ushuaia (Argentina)	54°50′S, 68°18′W; sea level	1 January 1995–31 December 2002	2492

*This article includes data from all stations except Puerto Rico and Trelew 2.

tered at 305 nm and 320 nm (UV-B), 340 nm and 380 nm (UV-A) and 400–700 nm (photosynthetically active radiation [PAR]). They provide valuable information on the spectral distribution of the solar radiation as it relates to ozone dynamics and other factors.

MATERIALS AND METHODS

Surface UV radiation is a function of several factors, such as the distance between the earth and sun, the levels of atmospheric gases and aerosols, the solar zenith angle (SZA), the cloud cover, the altitude and the surface albedo. Geometric factors (*i.e.* the SZA and the distance between the earth and sun) are responsible for pronounced and systematic variations in irradiance. For example, variation in the distance between the earth and sun produces an alteration in extraterrestrial radiation of 7% between the maximum distance at the beginning of July and the minimum distance at the beginning of January (23). Irradiance variation with respect to time of the day, latitude and season result from changes in the SZA. Cloud cover is an important factor to which short-term variability is attributed. Clouds attenuate the level of UV irradiance, although partly cloudy conditions have been associated with increases of up to 27% over levels for clear skies (24,25).

Ozone. Total column ozone levels were measured by Total Ozone Mapping Spectrometers, version 8, on Nimbus-7, Meteor-3, and Earth Probe satellites and data were provided by the North American Space Administration (NASA) Goddard Space Flight Center (13,14). We examined data obtained from January 1979 through December 2004; historical maximum, minimum and mean values for each Julian Day and annual cycle were determined. The mean annual total column level and its interannual variation were also determined. The global ultraviolet (GUV), which was originally located in Puerto Madryn, was moved to Trelew during 1998. Both cities are very close to each other (50 km apart); therefore, ozone data for Trelew were used in the analysis of the data obtained at both sites. Because NASA does not provide overpass values for Bariloche (41.01°S, 71.42°W), the closest grid point (lat 41.5°S, long 71.875°W) was selected.

To determine the annual cycle we used a procedure described in Wilks (15), which is a more general version of the Fast Fourier Transform (FFT) spectral analysis. FTT has the advantage that equidistant data are not needed because coefficients and phases corresponding to the harmonic components are obtained *via* multivariate analysis.

The annual component of a time series may be represented by the following cosine function:

$$y_t = \bar{y} + C_1 \cos\left(\frac{2\pi t}{n} - \varphi_1\right) \qquad \text{(Eq. 1)}$$

where y_t is the value obtained on day t, $\bar{y}$: is the mean value of the annual cycle, t is time, n is number of days in the annual cycle (in this case, 365 days), C_1 is amplitude of the annual cycle and φ_1 is the phase.

Equation 1 may be reformulated by taking into account that

$$\cos(\alpha - \varphi_1) = \cos(\varphi_1)\cos(\alpha) + \sin(\varphi_1)\sin(\alpha) \qquad \text{(Eq. 2)}$$

Also, after performing the following replacement

$$A_1 = C_1 \cos(\varphi_1)$$
$$B_1 = C_1 \sin(\varphi_1)$$

and the following change of variable

$$x_1 = \cos(\alpha)$$
$$x_2 = \sin(\alpha)$$

where

$$\alpha = (2\pi t/n)$$

(Eq. 1) is transformed into a regressive equation with two predictors, as follows:

$$y_t = \bar{y} + A_1 x_1 + B_1 x_2 \qquad \text{(Eq. 3)}$$

Usually, the annual cycle is not a pure cosine function. It is rather the sum of the first ($n = 365$), second ($n = 180$) and third ($n = 120$) harmonics. If this is taken into account and the procedure explained above is followed, a multivariate equation with six predictors is obtained that, when solved, provides the annual cycle. The independent term of (Eq. 3) corresponds to the mean of the annual cycle or continuous component in the FFT. To confirm that the first three harmonics were enough to represent the annual cycle, we performed a spectral analysis of the residuals (*i.e.* historical mean value minus the annual cycle value), which showed that the annual cycle had been totally removed. Also, we added a fourth harmonic and confirmed that it did not improve the annual cycle (data not shown).

To complete the analysis the mean annual total column ozone level was calculated. Also, we determined the mean (±SD) of the annual mean time series and the maximum and minimum values (and the years in which they occurred). The mean value of the annual means for 1980–1986 was included as reference. This period was selected as reference because it includes data from years in which the first satellite measurements were performed, when total column ozone levels were less affected by stratospheric depletion, and because it covers half a solar cycle (from a maximum to a minimum).

UV irradiances. In order to study irradiance climatologies, we analyzed the measurements provided by the Inter American Institute for Global Change Radiation Network (IAI RadNet). At present this network is composed of 10 multichannel radiometers (GUV 511, Biospherical Instruments Inc.), located in Chile, Argentina and Puerto Rico (Table 1). The instruments of the IAI RadNet were installed during the 1990s through the efforts of different nations and are still in operation. The geographical distribution of the stations allowed comparisons between tropical and sub-Antarctic regions. Data from 1995 to 2002 are presented in this analysis. Data from all stations except those in Puerto Rico and Trelew 2 are included.

The GUV511 is a temperature-stabilized multichannel radiometer that measures downwelling irradiances with moderately narrow bandwidth

channels (near 10 nm), centered at approximately 305, 320, 340 and 380 nm, plus PAR (400–700 nm) (16).

All instruments collected one measurement each minute 24 h per day. Raw data were processed by means of software provided by Biospherical Instruments and were modified by the Laboratory of UV and Ozone, CADIC, Ushuaia. During data processing the quality and consistency of the data were checked, night values (comprising instrument internal noise) were subtracted and calibration constants were applied. When the temperature controller failed or the operational temperature of the instrument differed from the temperature at the moment of the calibration, temperature corrections were applied to the calibration constants (17). Any observed changes in radiometric data were assumed to be linear. Therefore, calibration constants applied between two calibrations dates were calculated by linear interpolation between the two closest calibrations, unless an abrupt known change (*e.g.* during filter replacement) had occurred.

The GUV-511 apparatus were periodically sun calibrated, usually once per year, with a traveling reference GUV (RGUV) (16). The reference radiometer was calibrated under solar light (before and after movement) against the spectroradiometer SUV100 of the US National Science Foundation UV Radiation Monitoring Network (San Diego, CA) (18). During RGUV calibration the output voltage from each channel of the radiometer was related to the calibrated irradiance measured by the spectroradiometer at the nominal central wavelength of the channel. As a result, a calibrated monochromatic irradiance was obtained. Because of the bandwidth of the radiometer (10 nm), changes in the SZA and the ozone level introduce an error in the measurements performed by the RGUV, mainly in the 305 nm channel. These errors may be addressed by introducing the total column ozone level and the SZA in the calculation of the calibrated irradiance (19). In this way the calibration would be represented by a function rather than by a constant. Data from all calibrations during the period included in the present article were not available in order to back-calculate calibrations with the new improved procedure. Thus, the ozone and SZA corrections were not used in the analysis presented here. Tests performed during the calibration in 2000 indicated that the GUVs of the network had an error of 8–13%, based on the 305 channel and a SZA of $<60°$, with respect to the SUV-100 at San Diego, where the corrections for SZA and ozone were not applied. For channel 340, the error was $<5\%$ for all SZAs.

Irradiances were presented for channels 305 and 340 of the GUV-511. The first channel was chosen because it is the most sensitive to ozone changes and the second because it is independent of ozone variations and a good proxy for factors like cloud cover (20). Time-series analyses were based on daily maximum irradiance values. When no clouds are present, maximum irradiance occurs at solar noon; when clouds are present, larger irradiance values may occur at other times of the day. For each Julian Day we determined the historical maximum, minimum and mean irradiance values; the annual cycle was inferred on the basis of these values. The procedure for calculating the total column ozone annual cycle was slightly modified for irradiances. Because the seasonal variability in UV radiation is very pronounced, the annual cycle calculated for irradiance would present large errors in the winter, owing to the small weight that winter irradiance presents when solving the multivariate equation by means of the least squares method. In order to avoid this problem, the irradiance values were logarithmically transformed before solving the multivariate equation. The irradiance annual cycle is the result of the annual variation of several factors (*e.g.* the SZA, the distance between the earth and the sun and the ozone level). If, in (Eq. 1), y_t is expressed as the sum of the annual cycles (cosine functions) of two or more factors with different amplitude and phase and then they are decomposed as explained in the equations following (Eq. 1), the resulting multiregressive equation will have the same number of terms as (Eq. 3) but coefficients A_1 and B_1 and the independent term of the equation will vary, as a result of the amplitude and phase of the considered annual cycles. The methodology described by Wilks (15) and used in this study for the calculation of the irradiance annual cycle provided the annual cycle resulting from all of the parameters affecting the irradiance. As for ozone, the first three harmonics were used to construct the annual cycle and tests were performed to confirm that the annual cycle was well represented.

The monthly averaged daily integrated irradiance was calculated for months with data from ≥ 26 days. Cross-checking with data for equivalent months (without gaps) from different years revealed that the errors for the incomplete months would be $<10\%$, compared with the months without data gaps. This error is smaller than the dispersion observed between data without gaps from different years for a given month and site. To avoid inconveniences produced by the existence of small gaps in the irradiance data set, monthly means for each hour of the day were first calculated using the following equation:

$$I_h = \frac{\sum_{j=1}^{p} I_{jh}}{p}$$

where I_h is the monthly mean irradiance for time h (in $\mu W\ m^{-2}$), I_{jh} is the irradiance measured at day j and time h (in $\mu W\ m^{-2}$) and p is the number of days in the month with data for time h.

Then, the monthly averaged, daily integrated irradiance was obtained by summing data for all hours of the day and multiplying the results by the necessary constants to produce consistent units, because irradiance is in $\mu W\ m^{-2}$ and the daily integrated irradiance is in $J\ m^{-2}$. Negative values, which have no physical meaning and only reflect values of irradiance smaller than the internal noise of the instrument, were removed from the database before starting this calculation.

The ratio of the UV-B bands to the UV-A bands is of interest in biological and atmospheric studies. The ratio of wavelengths representing each UV band has been used as an index to highlight ozone variability (21,22). We chose the ratio of 305/340 nm over the UV-B/UV-A ratio because 305 nm is more sensitive to ozone and SZA variations, compared with UV-B (295–320 nm). Similarly, the 305/340 nm ratio is more sensitive to these variations, compared with the UV-B/UV-A ratio, and can be used to highlight temporal and geographical differences. Therefore, the annual cycle and latitudinal variability is expected to be more pronounced for the 305/340 nm ratio than for the UV-B/UV-A ratio.

Anomalies. For continuous meteorological variables, persistence (*i.e.* the tendency for weather in successive periods to be similar) is characterized in terms of serial correlations or temporal autocorrelations (15). We performed persistence studies based on time series of anomalies.

Normalized anomalies for total column ozone, channel 305 nm and channel 340 nm were calculated as deviations from the annual cycle by means of the following equation:

$$anomaly = \left(\frac{V_d - V_J}{V_J}\right)$$

where V_d is the time series value at date d and V_J is the annual cycle value at Julian Day J, corresponding to date d.

Usually, the anomaly is normalized by dividing it by the SD. In this case we preferred to use the value of the annual cycle for normalization because, as consequence of ozone depletion, the SDs for channel 305 and total column ozone are perturbed at higher latitudes.

Autocorrelation for ozone, 305 nm and 340 nm and cross-correlations between 305 nm and ozone and 340 nm for time lags of 1–7 days were performed.

RESULTS AND DISCUSSION

Surface UV radiation is a function of several factors, such as the distance between the sun and the earth, the concentration of atmospheric gases and aerosols, the SZA, the presence of clouds, the altitude and the surface albedo. Geometric factors (SZA and the distance between the earth and sun) are responsible for pronounced and systematic variations in irradiance. For example, the variation in the distance between the earth and the sun produces an alteration in extraterrestrial radiation of 7% (23), with a maximum distance at the beginning of July and a minimum distance at the beginning of January. Irradiance variations associated with time of the day, latitude and season result from changes in the SZA. Cloud cover is another important factor. Short-term variability in UV irradiance is attributed to this parameter. Clouds attenuate the UV irradiance except under broken cloud conditions, in which an increase of up to 27% above clear sky values can be observed (24,25).

Ozone

Ozone is the most important atmospheric gas that affects ground-level UV-B irradiance. When studying UV-B radiation, special interest is given to this gas, because of the depletion observed in

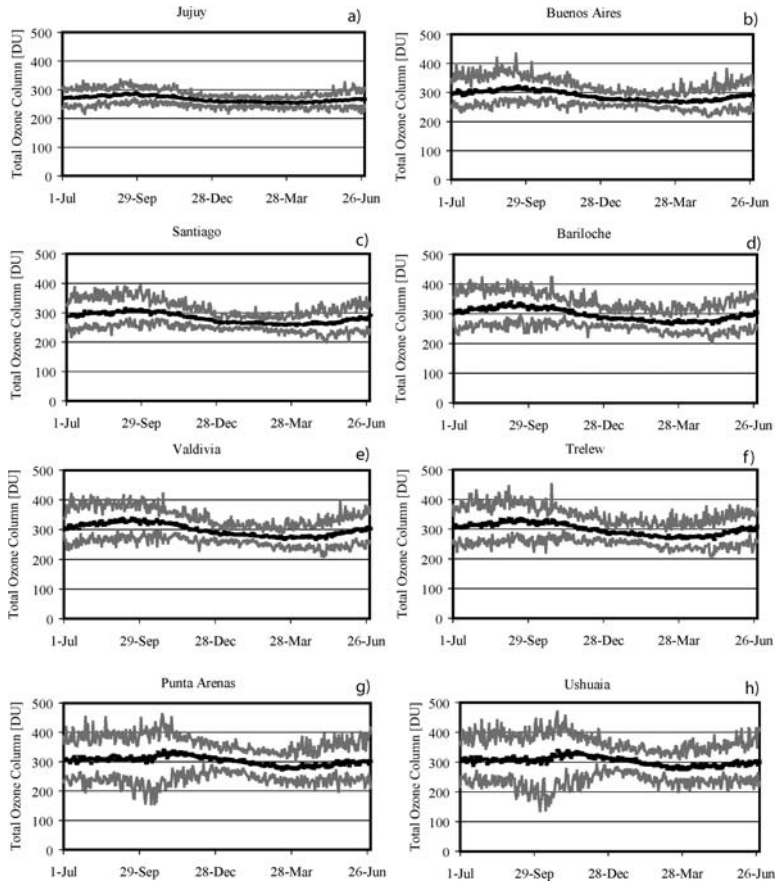

Figure 1. Total column ozone levels. Historical maximum (upper full grey line), minimum (lower full grey line), mean (dotted line) and annual cycle (full black line), calculated from maximum daily irradiance values, based on (Eq. 3), for the period 1979–2004.

recent decades (6–9). Ozone presents important temporal and geographical variations. Higher total column ozone is usually observed at higher latitudes and lower values are observed at the tropical regions (6). Main temporal variations of this parameter are based on season, which is more pronounced at high latitudes, and time of day. Other temporal changes are related to the quasi-biennial oscillation (QBO) (26–28), the 11 year sun spot cycle and the 27 day sun rotation (29–33).

Historical maximum, minimum and mean and annual cycle of total column ozone for each Julian Day between 1 January 1979 and 31 December 2004 are presented in Figure 1. In general, the annual cycle showed a maximum in late winter and spring, a minimum in late summer and autumn and a larger amplitude at higher latitudes, as expected. Several interesting points are worth highlighting. The seasonal and day-to-day variability were considerably smaller at Jujuy than at the other sites. At Punta Arenas and Ushuaia the sinusoidal pattern of the annual cycle looked broken. We attributed this to the overpass of the ozone hole and to low ozone air masses from Antarctica passing over the region. Furthermore, the ozone hole effect shifted the maximum value during the annual cycle in these 2 localities.

Table 2. Total ozone column. Mean and standard deviation of year mean for the period 1979–2004; maximum and minimum values of the time series, and year when they occurred; and mean of year mean 1980–1986, as a reference, are presented.

Site	Annual mean level ± SD, 1979–2004 (DU)	Maximum level (DU); year	Minimum level (DU); year	Mean level, 1980–1986 (DU)
Jujuy	267.36 ± 6.27	334.70; 1991	217.00; 2004	268.99
Buenos Aires	288.94 ± 8.71	433.80; 1979	216.40; 1997	291.85
Santiago	281.07 ± 8.01	391.00; 1983	200.40; 2004	283.37
Bariloche	296.83 ± 9.37	423.00; 1979	204.00; 2004	302.77
Valdiva	299.64 ± 8.89	421.30; 1979	209.80; 1997	304.92
Trelew	299.12 ± 9.23	451.40; 1979	208.30; 2004	305.31
Punta Arenas	302.98 ± 10.63	461.00; 1979	155.50; 2000	313.47
Ushuaia	302.42 ± 11.35	469.10; 1979	136.1; 2003	314.50

The mean annual total column ozone level showed the expected increase from tropical to high latitudes (Table 2). The difference between the mean for the series 1979–2004 and the mean for 1980–1986 (the reference period) was consistent with the observed latitudinal variation in ozone depletion. In general, the maximum total column ozone of the time series occurred during or close to the years of maximum solar activity and/or at the beginning of the time series, whereas the minimum level occurred during or close to years of minimum solar activity and/or towards the end of the time series. Data from Punta Arenas were exceptions, because 2000 corresponded to a maximum value of the solar cycle. The SD increased with latitude. Maximum and minimum values increased and decreased, respectively, with latitude. For all sites, the minimum values were <220 Dobson Units (DU) (which is considered as the limit of the spring Antarctic ozone hole over high latitudes, although the hole may be present over other regions or seasons, mainly during autumn, when the minimum value of the ozone annual cycle occurs). Jujuy had minimum annual total column ozone <220 DU

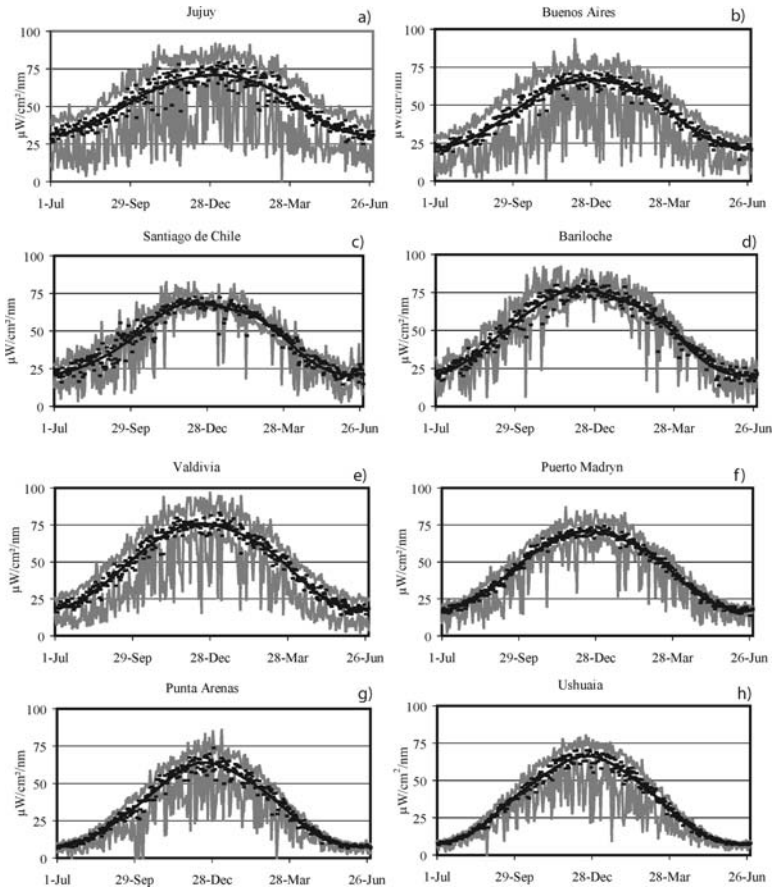

Figure 2. Irradiance channel 340. Historical maximum (upper full grey line), minimum (lower full grey line), mean (dotted line) and annual cycle (full black line), calculated from maximum daily irradiance values for the period 1995–2002, except for Bariloche, which includes values from 1998–2002.

in 1992, 1998 and 2004. These minima occurred during different seasons. Buenos Aires showed values <220 DU in1997; Santiago in 1986, 1996, 1997, 1998, 2002 and 2004; and Valdivia, Bariloche and Trelew in 1997 and 2004. In all these cases the minimum levels were recorded during autumn. Interestingly, in the last three stations, the minima did not coincide with the occurrence of the Antarctic Ozone hole. It was observed that values in 1997 were <220 DU at most stations. Fioletov *et al.* (34) reported record large negative deviations from pre-1980 for 1997 at 35–60°S latitude, which persisted once the QBO and the solar cycle were removed. Observations of the Halogen Occultation Experiment determined that record low ozone level observed in 1997 (at 20–40°S latitude) was mainly confined to the lower stratosphere (35).

The locations affected by the ozone hole presented different dynamics (6–9). Ushuaia showed values <220 DU every spring, starting in 1990; Punta Arenas had similar conditions except in 1993. Before 1990 Ushuaia had values of <220 DU almost every year, during winter or autumn, and such values were observed for Punta Arenas on a few occasions during the same seasons.

Irradiance

The irradiances in the UV-B and UV-A bands present differences in latitudinal and seasonal distribution. In addition, parameters affecting UV showed a large variety of combinations at the studied sites, which were reflected in the variability patterns.

Historical maximum, minimum, mean and annual cycles of daily maximum UV irradiance for the 340 nm channel (Fig. 2) showed there were slight differences in mean summer values between sites (range, 64–77 µW cm^{-2}). We attributed the small geographical variation of summer values to several factors. First, UV-A variation with SZA and, thus, with latitude is not as pronounced as that for shorter wavelengths (*i.e.* those in the UV-B range) because of molecular (Rayleigh) scattering. Second, large cities such as Santiago and Buenos Aires suffer from urban pollution (*i.e.* an aerosol burden) that may attenuate the radiation, which is almost completely absent in small towns such as Puerto Madryn. Altitude is an important factor, with increasing solar radiation in places as Jujuy and Bariloche. Rayleigh scattering and, in some cases, the increase in the albedo and the decrease in cloud cover associated with increased altitude all contribute to higher radiation levels. Finally, differences in cloud cover among locations may mask latitudinal differences (36) (as explained below). Winter mean values at the 340 nm channel, which ranged from 7 to 31 µW cm^{-2}, showed a more pronounced latitudinal variation than those in the summer. This variability is partially associated with the more rapid variation of the cosine of SZA among locations at this time of the year.

The variation in the cosine of the SZA might explain the increase of seasonal variability with latitude, exhibiting a summer-to-winter ratio of 2.1 in Jujuy and 9.4 in Ushuaia (Fig. 3). In addition, cloudiness affected variability at the local scale. Puerto Madryn showed the lowest and Jujuy the highest day-to-day variability in this band. Puerto Madryn has a semiarid condition, whereas Jujuy has rainy summers. Furthermore, Bariloche and Santiago presented the smallest variability during summer. Both areas are characterized by dry summers.

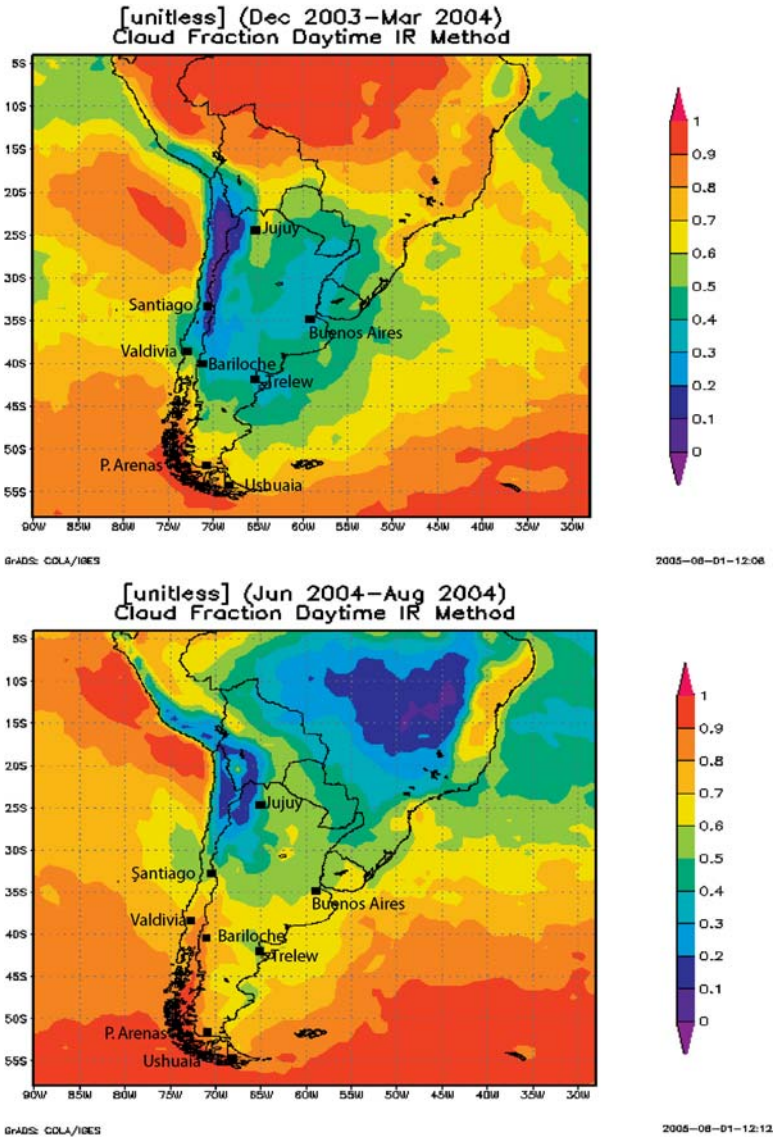

Figure 3. Cloud cover during summer and winter in South American region, where data from the GUV-511 radiometers analyzed in this study were obtained.

Geographical differences and the annual cycle amplitude were more pronounced at the 305 nm channel than at the 340 nm channel, as expected (Fig. 4). Summer mean values varied from 5 μW cm^{-2} at Ushuaia to 10 μW cm^{-2} at Jujuy, and winter mean values ranged from 0.04 μW cm^{-2} at Ushuaia to 2.3 μW cm^{-2} at Jujuy. As a direct consequence of variations associated with SZA and ozone level, lower latitudes had larger values during all seasons and a smaller amplitude of the annual cycle. Mean values for the summer-to-winter ratio were 4.4 at Jujuy and 125 at Ushuaia.

The 305 nm channel is affected by all of the factors mentioned for the 340 nm band and, in addition, by total column ozone. In some cases these factors may compete or result in additive effects. For example, the presence of clouds can mask the effect of ozone depletion. Strong ozone depletion produced while the ozone hole was passing overhead, during cloudy conditions and in conjunction with high SZAs can, on clear days, produce lower irradiances than weaker ozone depletions near the summer solstice (37). To determine which factors were responsible for the variability observed with the 305 nm channel, we compared the irradiance at both wavelengths with the ozone level during the same period. We observed that the springtime variability at the historical maximum in Punta Arenas and Ushuaia was mainly the result of low total column ozone associated with the presence of the ozone hole vortex (Figs. 1–3). Similarly, places such as Valdivia, Puerto Madryn and Bariloche showed spring irradiance values affected by low ozone amounts. This may be inferred by the fact that the maximum and mean values showed an increase at the 305 nm channel but not the 340 nm channel.

Monthly averaged, daily integrated irradiance values for channel 305 (Fig. 5) were extreme in December and January and in June and July, as expected. All sites except Punta Arenas and Ushuaia showed similar summer values, which oscillated between 1 and 1.7 kJ/m^2; daily integrated values at Punta Arenas and Ushuaia during the summer were *ca* 50% less (0.6–0.9 kJ m^{-2}). To explain this variability we first need to consider that the duration of daylight varies considerably among stations. At Jujuy the duration varies from 10.5 h in June to 13.5 h in December. At Ushuaia the duration varies from 7 to 17 h. Second, analysis of channel 340 nm and total column ozone showed that the observed interannual variability was related to both ozone and cloud cover variations,

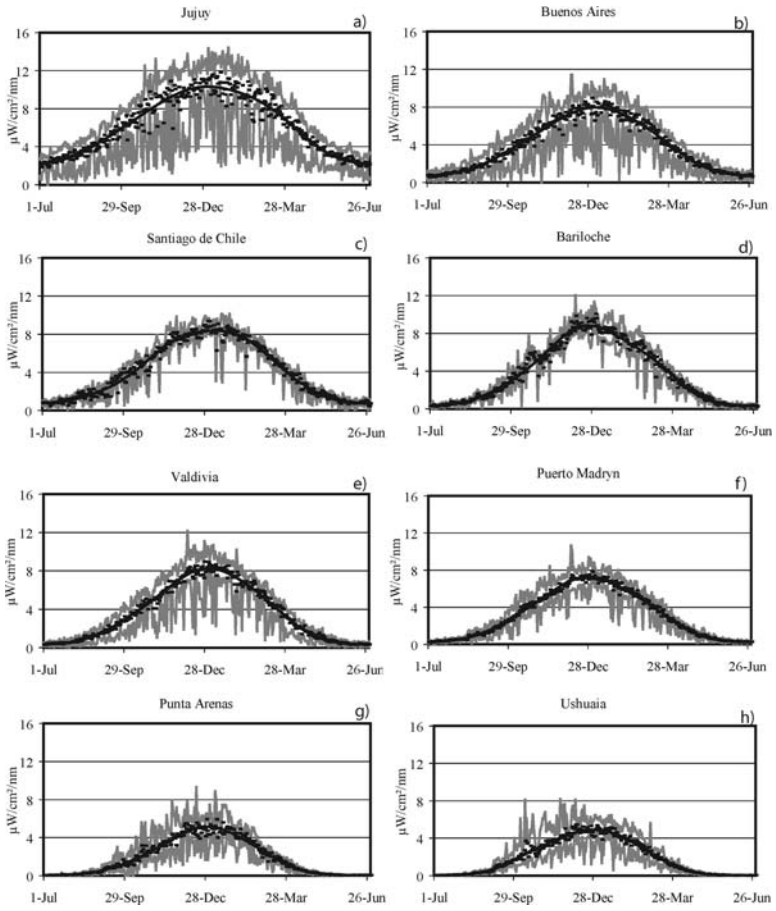

Figure 4. Irradiance channel 305. Historical maximum (upper full grey line), minimum (lower full grey line), mean (dotted line) and annual cycle (full black line), calculated from maximum daily irradiance values for the period 1995–2002, except for Bariloche, which includes values from 1998–2002.

although the effect of ozone was less pronounced than that observed for instantaneous values (as explained below). Other factors, such as aerosols, could have influenced the interannual variability but this could not be confirmed in the present analysis. In contrast to summer values there was a larger latitudinal variation in daily integrated values during the winter (ranging from 0.2 kJ m^{-2} at Jujuy to 0.004 kJ m^{-2} at Ushuaia), because of the effect of SZA, ozone and duration of daylight. This resulted in a seasonal ratio of 7 at Jujuy and of >150 at Ushuaia.

Monthly averages mask some interesting features in the data. Instantaneous values at the 305 nm channel showed that, during spring, the irradiance was highly affected by ozone depletion at the southern stations. When monthly values were considered, the effect vanished at Ushuaia and Punta Arenas (Fig. 5).

Ratio 305/340

The ratio of a wavelength or narrow band in the UV-B and in the UV-A is of interest for biological studies. In some organisms UV-A contributes to the recovery from the damage produced by UV-B (38,39). Also, this ratio is relevant for atmospheric research, because the parameters that affect UV irradiance have different spectral patterns. For example, 305 nm presents a more pronounced variation with SZA than 340 nm (compare seasonal cycles in Fig. 2 with Fig. 3). The ratio of 305 to 340 is then a function of SZA, resulting in a systematic variability with latitude and seasons (22). Cloud cover has a slight spectral dependence; the ratio removes most of the cloud effect (21). Furthermore, changes in total column ozone produce abrupt changes in the ratio as consequence of ozone absorption spectral pattern (21). Therefore, this ratio can highlight variations in ozone levels, and the effects of cloud cover can be minimized (21,22).

Historical maximum, minimum, mean and annual cycle of the 305/340 nm ratio at solar noon are shown in Figure 6. Solar noon values were considered, because use of the ratio removed most of the effects due to clouds.

Latitudinal variation showed a doubling of the ratio between Jujuy and Ushuaia in summer, and the ratio was even higher in winter. At Jujuy the extreme values of the annual cycle were 0.15 and 0.07 and at Ushuaia the extreme values were 0.08 and 0.005. Another interesting feature can be seen during springtime, when anomalously large values were observed in Ushuaia and Punta Arenas that showed good agreement with the presence of low ozone levels. At Punta Arenas the largest value was 0.14 on 21 November 1999, with a total column ozone level of 216.4 DU. Slightly lower values (0.13) were present on 18 December 1996 (237.3 DU), 22 October 1998 (203.6 DU), 8 December 1998 (229.1 DU), 12 October 2000 (155.5 DU) and 1 November 2002 (215 DU). At Ushuaia the maximum was 0.17 and was detected on 12 October 2000 (139 DU) and 0.16 was detected on 14 November 1997 (207 DU). It may be observed that a mild ozone depletion at the end of springtime can produce high ratios similar to those associated with pronounced ozone depletion at the midpoint of springtime. This is a consequence of the increase in the ratio associated with SZA as the season progresses.

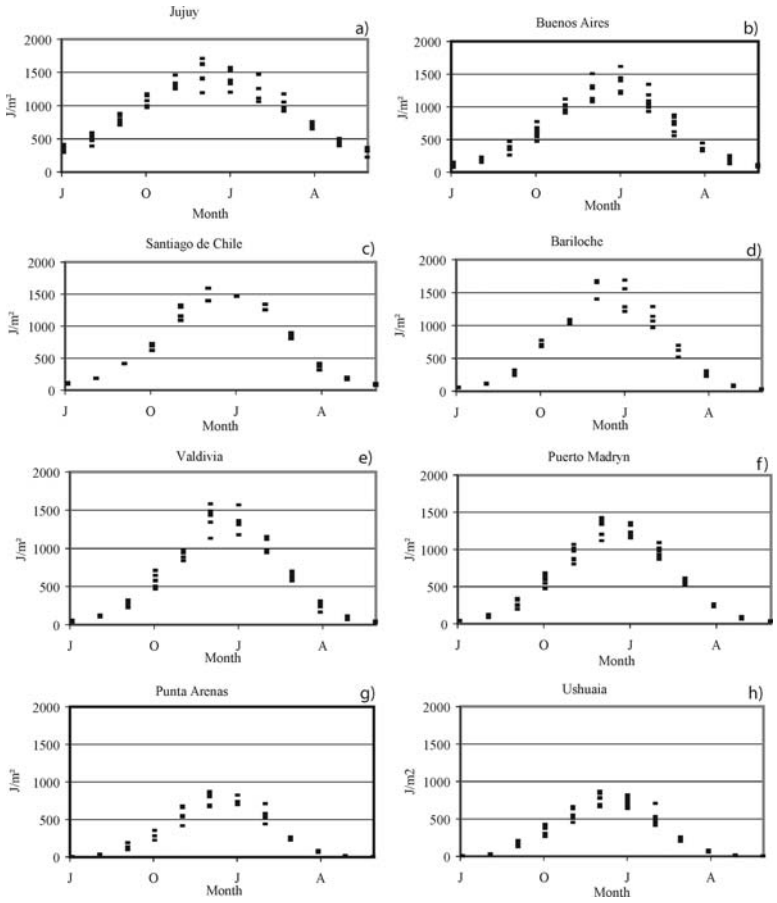

Figure 5. Monthly average of the daily integrated irradiance for the 305 nm channel.

Anomalies

We studied the persistence of anomalies because this is an interesting factor for biological and atmospheric research. In biology, the combination of this persistence and relatively high irradiance may influence cumulative UVR effects, whereas in atmospheric studies large values of persistence allows for better forecasting and the possibility of developing autoregressive models.

Table 3 shows coefficient R for autocorrelations (at 1 day lag) and cross-correlations (at zero lag). The autocorrelations at a lag of 1 day for total column ozone were relatively large (between 0.69 and 0.63). For a 2 day lag the autocorrelations oscillated between 0.58 and 0.42; for longer lags autocorrelations approached 0.39 in Jujuy and ranged from 0.20 to 0.14 at the other sites (in all cases the values were statistically significant [$\alpha = 0.05$]).

Autocorrelations for irradiance at the 340 nm channel at a lag of 1 day were comparatively small, with the largest values at Jujuy (0.27), Buenos Aires (0.30) and Bariloche (0.27). At other sites they varied between 0.19 and 0.14. For longer lags the autocorrelations were very small and, in most cases, not statistically significant. For channel 305 autocorrelations at a lag of 1 day ranged from 0.36 to 0.27 and were considerably larger at Bariloche (0.43), Punta Arenas (0.43) and Ushuaia (0.50); at longer lags the autocorrelations decayed rapidly.

Cross-correlations between channels 305 and 340 varied widely by site at zero lag. Smaller values were observed at higher latitudes. At Trelew, Bariloche, Punta Arenas and Ushuaia the values varied between 0.64 and 0.48. At other sites they varied between 0.94 and 0.79. These values reflect the percentage of variability at channel 305 produced by cloud cover, albedo and aerosols changes. For lags of ≥ 1 day the autocorrelations diminished rapidly.

Cross-correlation between channel 305 and total column ozone also varied geographically. At zero lag the cross-correlation for Jujuy was 0.17, whereas for Ushuaia the value was 0.75. The other stations had values between those of Jujuy and Ushuaia that depended on latitude. These results are consistent with the relationship between channel 305 nm and ozone, which becomes more important at higher latitudes. All values decayed for longer time lags.

The results imply a larger persistence of the total column ozone level, compared with irradiance. Channel 340 showed a much smaller persistence than channel 305 at all latitudes, which is interpreted as the lack of ozone influence in this band. Furthermore, the relationship between 305 and 340 nm and between 305 nm and ozone indicated that factors such as cloud cover tend to dominate the variability of 305 nm in northern sites and of ozone in southern sites.

CONCLUSIONS

In general, total column ozone time series showed the maximum value during or close to the years of maximum solar activity and/or at the beginning of the time series, whereas the minimum value was detected during or close to years of minimum solar activity and/or toward the end of the time series.

Minimum annual total column ozone levels <220 DU were observed at all sites, in most cases during autumn. Jujuy (24.17°S, 65.02°W) showed low ozone at different seasons. Ushuaia and

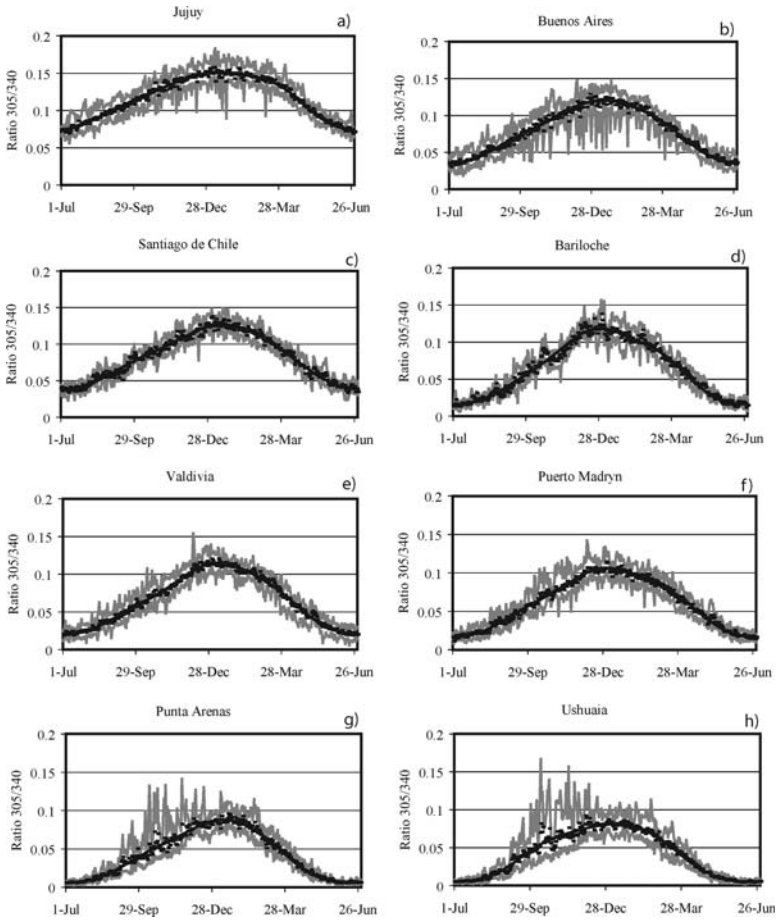

Figure 6. Ratio channel 305/channel 340. Historical maximum (upper full grey line), minimum (lower full grey line), mean (dotted line) and annual cycle (full black line), calculated from maximum daily irradiance values for the period 1995–2002, except for Bariloche, which includes values from 1998–2002.

Punta Arenas presented minima of <220 DU every spring, beginning in 1990; before 1990 these levels were present in winter and autumn.

Irradiance in the UV-B channel and total column ozone varied with latitude, as expected. The UV-A channel showed a more complex geographical pattern, because it was affected by local atmospheric conditions.

Latitudinal differences and the amplitude of the annual cycle were more pronounced in the 305 nm channel, compared with the 340 nm channel, as consequence of the effect of SZA and ozone.

Table 3. Autocorrelation (Auto) and cross-correlation (Cross) R coefficients for anomalies.*

Site	Auto ozone (lag = 1 day)	Auto 340 nm (lag = 1 day)	Auto 305 nm (lag = 1 day)	Cross 305–340 (lag = 0 days)	Cross 305–Oz (lag = 0 days)
Jujuy	0.69	0.27	0.33	0.94	0.17
Buenos Aires	0.69	0.30	0.36	0.87	0.32
Santiago	0.69	0.15	0.27	0.83	0.28
Bariloche	0.64	0.27	0.43	0.64	0.55
Valdiva	0.64	0.11	0.27	0.79	0.34
Trelew	0.63	0.14	0.36	0.60	0.62
Punta Arenas	0.67	0.19	0.43	0.58	0.61
Ushuaia	0.67	0.07	0.50	0.48	0.75

*$\alpha = 0.05$.

Monthly averaged daily integrated irradiance for channel 305 showed similar values at all sites except Punta Arenas and Ushuaia, whereas winter values showed a larger latitudinal variation. These results were a consequence of the effect of SZA, ozone and daylight duration.

Mild ozone depletion at the end of spring can produce similar 305/340 ratios than those under pronounced ozone depletion in the middle of spring. This results from the increase in the ratio as the SZA diminishes.

Total column ozone anomalies showed a larger persistence than did irradiance at 305 and 340 nm. Irradiance at 340 nm showed the smallest persistence. The relationships between 305 and 340 nm anomalies and between 305 nm and ozone anomalies indicated that factors such as cloud cover tend to dominate 305 nm variability in northern sites and ozone variability in southern sites.

Acknowledgements—This study was funded by a grant from the Inter-American Institute for Global Change (CRN-026). We thank Dr. Luis Orce for leading the installation of and operating the instruments at Jujuy, Buenos Aires, Puerto Madryn and Ushuaia when the Argentinean network was first created; Drs. McPeters and Herman, NASA/GSFC, for providing total column ozone data; Jim Ehramjian, James Robertson and the UV group (Biospherical Instruments Inc.) for calibrating the GUVs and RGUV; Dr. Paula Vigliarolo for contributing to the extraction of total column ozone for Bariloche; Drs. San Román, Buitrago, Labraga, Hebling and Dieguez for collaborating in data collection at Ushuaia, Jujuy, Puerto Madryn, Playa Unión and Bariloche; and Centro Austral de Investigaciones Cientificas, Consejo Nacional de Investigaciones Científicas y Técnicas, Argentina.

REFERENCES

1. Farman, J. C., B. G. Gardiner and J. D. Shanklin (1985) Large losses of total ozone in Antarctica reveals seasonal ClOx/NOx interaction. *Nature* **315**, 207–210.
2. United Nations Environmental Program (1991) *Environmental Effects of Ozone Depletion: 1991* (Edited by J. C. van der Leun, X. Tang and M. Tevini). United Nations Environmental Programme, Nairobi, Kenya.
3. United Nations Environmental Program (1994) *Environmental Effects of Ozone Depletion: 1994* (Edited by J. C. van der Leun, X. Tang and M. Tevini). United Nations Environmental Programme, Nairobi, Kenya.
4. United Nations Environmental Program (1998) *Environmental Effects of Ozone Depletion: 1998* (Edited by J. C. van der Leun, X. Tang and M. Tevini). United Nations Environmental Programme, Nairobi, Kenya.
5. United Nations Environmental Program (2002) *Environmental effects of ozone Depletion: 2002* (Edited by J. C. van der Leun, X. Tang and M. Tevini). United Nations Environmental Programme, Nairobi, Kenya.
6. World Meteorological Organization (1992). *Scientific Assessment of Ozone Depletion: 1991. United Nations Environment Program, World Meteorological Organization. Global Ozone Research and Monitoring Project* (Edited by D. L. Albritton, R. T. Watson and P. J. Aucamp). WMO/UNEP, Nairobi, Kenya.
7. World Meteorological Organization (1995) *Scientific Assessment of Ozone Depletion: 1994. United Nations Environment Program, World Meteorological Organization. Global Ozone Research and Monitoring Project* (Edited by D. L. Albritton, R. T. Watson and P. J. Aucamp). WMO/UNEP, Nairobi, Kenya.
8. World Meteorological Organization (1999) *Scientific Assessment of Ozone Depletion: 1998. United Nations Environment Program, World Meteorological Organization. Global Ozone Research and Monitoring Project* (Edited by D. L. Albritton, R. T. Watson and P. J. Aucamp). WMO/UNEP, Nairobi, Kenya.
9. World Meteorological Organization (2003) *Scientific Assessment of Ozone Depletion: 2002. United Nations Environment Program, World Meteorological Organization. Global Ozone Research and Monitoring Project* (Edited by D. L. Albritton, R. T. Watson and P. J. Aucamp). WMO/UNEP, Nairobi, Kenya.
10. Cede, A., M. Blumthaler, E. Luccini, R. Piacentini and L. Nuñez (2002) Effects of clouds on erythemal and total irradiance as derived from data of the Argentine Network. *Geophys. Res. Lett.* **29**, 2223 (DOI:10.1029/2002GL015708).
11. Cede, A., E. Luccini, L. Nuñez, R. Piacentini and M. Blumthaler (2002) Monitoring of erythemal irradiance in the Argentine ultraviolet network. *J. Geophys. Res.* **107**, 4165 (DOI:10.1029/2001JD001206).
12. Pazmiño, A., S. Godin-Beekmann, M. Ginzburg, S. Bekki, A. Hauchecorne, R. Piacentini and E. Quel (2005) Impact of Antarctic polar vortex occurrences on total ozone and UVB radiation at southern Argentinean and Antarctic stations during 1997–2003 period. *J. Geophys. Res.* **110** (DOI:10.1029/2004JD005304).
13. Herman, J. (2004) TOMS ADEOS. *NASA/GSFC*, Version 8. Available at: http://toms.gsfc.nasa.gov/ozone/ozoneother.html. Accessed on 8 March 2005.
14. Mc Peters, R., and E. Beach (2004) TOMS Nimbus 7, Meteor 3 and Earth Probe. *NASA/GSFC*, Version 8. Available at: http://toms.gsfc.nasa.gov. Accessed on 8 March 2005.
15. Wilks, D. S. (1995) Time series. In *Statistical Methods in the Atmospheric Sciences, International Geophysics Series,* Vol. 59 (Edited by R. Dmowska and J. R. Holton). Academic Press, San Diego.
16. Booth, R., T. Mestechkina and J. H. Morrow (1994) Errors in the reporting of solar spectral irradiance using moderate band-width radiometers and experimental investigation. In *Ocean Optics*, Vol. XII, 13–15 June, 1994, Bergen, Norway (Edited by J. S. Jaffe), pp. 654–663. Proceedings of SPIE. Bellingham, Washington, USA.
17. Booth, R. (1998) *Application Note: Temperature Coefficients in PUV and GUV Radiometers and Suggested Compensation Methods.* Biospherical Instruments Inc., San Diego, CA.
18. Booth, C. R., T. B. Lucas, J. H. Morrow, C. S. Weiler and P. A. Penhale (1994) The United States National Science Foundation's Polar Network for monitoring ultraviolet radiation. In *Ultraviolet Radiation in Antarctica Measurements and Biological Effects. Antarctic Research Series,* Vol. 62 (Edited by C. Susan Weiler and Polly A. Penhale), pp. 17–37. American Geophysical Union, Washington, DC.
19. Diaz S. B., C. R. Booth, R. Armstrong, C. Brunat, S. Cabrera, C. Camilion, C. Cassiccia, G. Deferrari, H. Fuenzalida, C. Lovengreen, A. Paladini, J. Pedroni, A. Rosales, H. Zagarese and M. Vernet (2005) Multi-channel radiometers calibration: A new approach. *Appl. Opt.* **44**, 5374–5380.
20. Díaz S., G. Deferrari, D. Martinioni and A. Oberto (2000) Regression analysis of biologically effective integrated irradiances versus ozone, clouds and geometric factors. *J. Atmos.-Solar Terr. Phys.* **62**, 629–638.
21. Lubin, D. and J. Frederick (1989) Measurements of Enhanced Springtime Ultraviolet Springtime Radiation at Palmer Station. *Geophys. Res. Lett.* **16**, 783–785.
22. Frederick, J. E., S. B. Diaz, I. Smolskaia, W. Esposito, T. Lucas and C. R. Booth (1994) Ultraviolet solar radiation in the high latitudes of South America. *Photochem. Photobiol.* **60**, 356–362.
23. Frölich, C. (1987) Variability of the solar ''constant'' on time scales of minutes to years. *J. Geophys. Res.* **92**, 796–800.
24. Estupinan, J. G., S. Raman, G. H. Crescenti, J. J. Streitcher and W. F. Barnard (1996) The effects of clouds and haze on UV-B radiation. *J. Geophys. Res.* **101**, 807–816.
25. Frederick, J. and H. Steele (1995) The transmission of sunlight through cloudy skies: An analysis based on standard meteorological information. *J. Appl. Meteorol.* **34**, 2755–2761.
26. Huang, T. Y. W. (1986) The impact of solar radiation on the quasi-biennial oscillation of the ozone in the tropical stratosphere. *Geophys. Res. Lett.* **23**, 3211–3214.
27. Randell, W. J. and F. Wu (1996) Isolation of the ozone QBO in SAGE II data by singular-value decomposition. *J. Atmos. Sci.* **53**, 2546–2559.
28. Zerefos, C, C. Meleti, D. Balis, K. Tourpali and A. F. Bais (1998) Quasi-biennial and longer-term changes in clear sky UV-B solar irradiance. *Geophys. Res. Lett.* **25**, 4345–4348.
29. Callis, L. B., M. Natarajan and J. D. Lambeth (2000) Calculated upper stratospheric effects of solar UV flux and NO_Y variations during the 11-year solar cycle. *Geophys. Res. Lett.* **27**, 3869–3872.
30. Chandra, S. and R. D. Mc Peters (1994) The solar cycle variation of ozone in the stratosphere inferred from Nimbus 7 and NOAA 11 satellites. *J. Geophys. Res.* **99**, 20 665–20 671.
31. Lean, J. L., G. J. Rottman, H. L. Kyle, T. N. Woods, J. R. Hickey and L. C. Puga (1997) Detection and parameterization of variations in solar mid- and near-ultraviolet radiation (200–400 nm). *J. Geophys. Res.* **102**, 29 939–29 956.
32. Zhou, S., G. J. Rottman and A. J. Miller (1997) Stratospheric ozone response to short- and intermediate-term variations of solar UV flux. *J. Geophys. Res.* **102**, 9003–9011.
33. Zhou, S., A. J. Miller and L. L. Hood (2000) A partial correlation analysis of the stratospheric ozone response to 12-day solar UV variations with temperature effect removed. *J. Geophys. Res.* **105**, 4491–4500.
34. Fioletov, V., G. Bodeker, A. Miller, R. Mc Peters and R. Stolarski (2002) Global and zonal total ozone variations estimated from ground-based and satellite measurements: 1964–2000. *J. Geophys. Res.* **107**, 4647 (DOI:10.1029/2001JD001350).
35. Cordero, E. and T. Nathan (2002) An examination of anomalously low column ozone in the Southern Hemisphere midlatitudes during 1997. *Geophys. Res. Lett.* **29**, 1123 (DOI:0.1029/2001GL013948).
36. Díaz, S. B., G. Deferrari, R. Booth, D. Martinioni and A. Oberto (2001) Solar irradiances over ushuaia (54.49°S, 68.19°W) and San Diego (32.45°N, 117.11°W) geographical and seasonal variation. *J. Atmos. Solar Terr. Phys.* **63**, 310–320.
37. Díaz, S. B., C. R. Booth, T. B. Lucas and I. Smolskaia (1994) Effects of ozone depletion on irradiances and biological doses over Ushuaia. In *Impact of UV-B Radiation on Pelagic Freshwater Ecosystems* (Edited by C. E. Williamson and H. E. Zagarese). *Archiv. Fur Hydrobiologie. Ergebnisse de Limnologie* **43**, 115–122.
38. Caldwell, M. M., L. B. Camp, C. W. Warner and S. D. Flint (1986) Action spectra and their key role in assessing biological consequences of solar UV-B radiation change. In *Strartospheric Ozone Reduction, Solar Ultraviolet Radiation and Plant Life* (Edited by R. C. Worrest and M. M. Caldwell), pp. 87–111. Springer-Verlag, Berlin.
39. Neal, P. and D. Kieber (2000) Assessing biological and chemical effects of UV in the marine environment spectral weighting functions. In *Causes and Environmental Implications of Increase UV-B Radiation* (Edited by R. E. Hester and R. M. Harrison). Issues in Environmental Science and Technology, No. 14. The Royal Society of Chemistry, Cambridge, UK, 61–83.